Regionalized Compensation Method for Nonlinear Error Control

Wei Wei
Qingchun Tang (gxtangqingchun@163.com)
Hunan University
Yutao Wang
Taizi Wang
Chenyang Zhang
Yingguang Pan

Research Article

Keywords: Five-axis linkage, Nonlinear error, Regional compensation optimization, Postprocessing, Turbine blade

Posted Date: May 25th, 2022

DOI: https://doi.org/10.21203/rs.3.rs-1646216/v1

Regionalized Compensation Method for Nonlinear Error Control

WeiWei[1], QingchunTang*[1], YutaoWang*[2], and TaiziWang[1]， ChenyangZhang[1], YingguangPan[1]

(1. College of Innovation and Entrepreneurship, Guangxi University of Science and Technology, Liuzhou, 545006, China

2. College of Mechanical Engineering, Donghua University, Shanghai, 201620, China)

Email: gxtangqingchun@163.com; 1040831715@qq.com

Abstract Although the five-axis machine tool presents excellent advantages of high-speed, -efficiency, and -precision machining of complex curved surface parts (impeller and blade), its actual motion demonstrates nonlinear principle error due to the participation of the rotating axis. Traditional methods, such as linear interpolation, Rotation Tool Centre Point(RTCP), and tool point optimization, can effectively control nonlinear errors despite their limitations. A regional compensation optimization method is proposed in this study to solve nonlinear error problems effectively in five-axis machining of complex curved surface parts. First, feature points of the complex free-form surface are identified, and regions are divided to distinguish the compensation optimization algorithm of each interval. Second, JAVA language is applied to develop a special postprocessor with nonlinear error partition compensation module. Finally, the BV100 machine tool is used as the experimental platform, and a turbine blade is utilized as the specimen for simulation and cutting experiments. Results showed that the surface quality and contour accuracy of machined parts improved when the nonlinear error regional compensation optimization algorithm is used.

Keywords Five-axis linkage, Nonlinear error, Regional compensation optimization, Postprocessing, Turbine blade

1 Introduction

Five-axis machine tools are widely used in aviation, aerospace, and automotive fields and other industries due to their advantages of high flexibility, degree of freedom, and precision and significant effect on the processing of high-precision curved surfaces [1-5]. However, compared with that of traditional three-axis machine tools, the increase of two rotational degrees of freedom of five-axis machine tools results in many technical issues in practice because it increases not only the flexibility of tool processing but also the complexity of the machine tool structure and difficulty of machine tool kinematics analysis [6-9]. Tool center trajectory will deviate from the theoretical trajectory and result in nonlinear errors, which will reduce surface precision of complex curved surface parts, due to the participation of two rotation axes. Many studies have primarily focused on the following fields to solve the problem of nonlinear error compensation of five-axis machine tools:

First, linear interpolation [10-12]. The nonlinear error is weakened by controlling the tool step length. However, a large increase in the number of programs due to an excessive reduction of the step length affects the NC system by prolonging the processing time and is not conducive to

commercial economic benefits.

Second, rotary tool center point (RTCP) method. This method reduces the nonlinear error by controlling the tool center to be in the planned path. Nonlinear error studies based on the RTCP method have been successfully used [13-15]. For example, Hang et al. [16] verified the effectiveness of the RTCP method through MATLAB simulation to analyze the kinematics of a double-turntable five-axis machine tool. Shi et al. [17] implemented real-time interpolation planning for five-axis maximum feed speed based on RTCP algorithm, and the experimental results showed that this method can effectively improve the surface quality of parts. Although the RTCP algorithm can effectively control nonlinear error, its implementation method is very expensive because it involves an advanced NC system.

Third, tool point position optimization method. This method reduces the nonlinear error by controlling the tool point trajectory [18-22]. Zhang et al. [23] proposed the SSALI method to avoid tool positioning beyond the theoretical programming plane. Li et al. [24] put forward a cubic spline interpolation and data density-integrated tool path optimization method to avoid overcutting phenomenon. Wu et al. [25] used harmonic function to construct a nonlinear error model and error compensation mechanism and verified its effectiveness through MATLAB simulation analysis. Although these methods can effectively reduce the nonlinear error, they can easily cause the phenomenon of corner or round corner overcutting because only the compensation of tool tip position is considered and whether the change of tool attitude meets the optimal cutting conditions is ignored.

Fourth, tool swing amplitude optimization method. This method controls the nonlinear error by adjusting the swing amplitude of adjacent points of the tool tip [26-32]. Fan et al. [33,34] proposed an optimization algorithm for cutter axis vector plane interpolation. Hong et al. [35] put forward a tool direction generation method based on surface triangular mesh. Although these methods can effectively prevent overcutting and improve the surface quality of parts when the tool rotation angle changes remarkably, they ineffectively compensate for nonlinear errors when adjacent tool axis vectors are in linear ratio or the tool feed direction is on the vertical plane.

To sum up, existing studies have mainly focused on nonlinear error compensation under a single factor constraint. However, a single nonlinear error processing method is unable to solve nonlinear error problems in the manufacturing process of complex curved surfaces effectively. A regional compensation optimization algorithm is proposed in this study to solve these problems. This manuscript contains the following research contents: First, compensation optimization algorithms for slow and sudden changes of the tool axis vector direction are established. Second, the recognition algorithm model is proposed to recognize the feature region on the tool path of complex curved surface while selecting different trajectory optimization algorithms according to the set recognition parameters. Finally, the BV100 machine tool and a turbine blade are used as the experimental platform and specimen, respectively. The experimental results showed that the proposed nonlinear error regional compensation method can improve the surface accuracy of machined parts in processing complex curved surfaces through simulation and actual cutting experiments.

2 Mechanism of nonlinear error

Although many types of five-axis CNC machine tools based on different kinematic configurations

are available, nonlinear errors caused by the rotating axis are consistent in the mechanism. The BV100, a five-axis machine tool with a typical double-swing table structure, is used as the experimental platform in this study to examine the mechanism of nonlinear error. Figure 1 shows the local coordinate system of the BV100 machine tool. Mathematical expressions of each motion axis of BV100 according to the preliminary research results [14] are presented as follows:

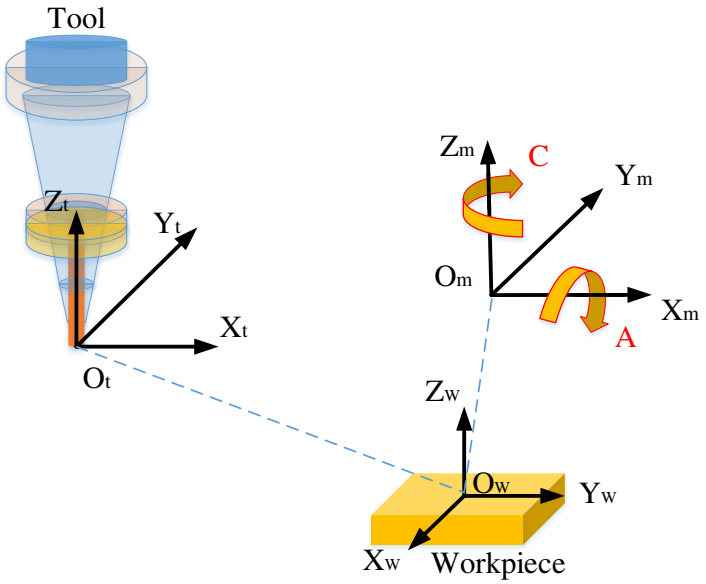

Fig. 1 Local coordinate system of BV100 five-axis machine tool

$$\begin{cases} X = (x_t + n_x)\cos C + (y_t + n_y)\sin C \\ Y = -(x_t + n_x)\sin C\cos A + (y_t + n_y)\cos C\cos A + (z_t + n_z)\sin A \\ Z = (x_t + n_x)\sin C\sin A - (y_t + n_y)\cos C\sin A + (z_t + n_z)\cos A \\ A = k_a \times \arccos(k) \quad k_a = 1, -1 \\ C = \arctan(i/j) - k_c\pi \quad k_c = 0, 1 \end{cases} \tag{1}$$

where X, Y, Z, A, and C are expressions of the drive value of each axis of the machine tool; (x_t, y_t, z_t) and (i, j, k) are the position and direction vector of the tool point in the workpiece coordinate system, respectively; and n_x, n_y, and n_z are structural parameters of the machine tool.

The five-axis machine tool processing aims to recognize the movement instruction through data in the tool position file using the postprocessing software and execute actual machining. As shown in Fig. 2, the solid line that connects two blue circles represents the ideal trajectory of the machine tool coordinate system and the solid line with red asterisks represents the actual trajectory of the machine tool coordinate system. The actual machining process of the machine tool clearly showed that the actual trajectory is a spatial curve form due to the linear interpolation method of each axis and the deviation from the ideal linear trajectory produces nonlinear errors. The vertical projection distance of the solid line with red asterisks to the solid line that connects two blue circles is the nonlinear error value.

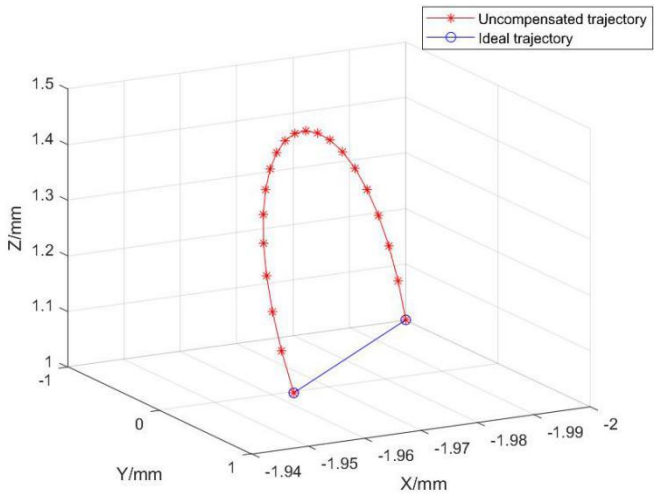

Fig. 2 Nonlinear error mechanism

3 Traditional nonlinear error processing algorithm

3.1 Harmonic function algorithm

Wu et al. [25] proposed a nonlinear error prediction and compensation principle based on an analytic model for slow cutter axis vector transformation. The proposed principle is divided into a prediction model and a compensation mechanism that represent the prediction of nonlinear error value and the establishment of the compensation mechanism on the basis of the predicted value, respectively. The specific mathematical expressions is expressed as follows:

$$L(t)=\sum_{1}^{n}A_i\cdot\sin(kt)+B_i\cdot\cos(kt)(n=1,2,3\mathrm{L}\ \ m) \tag{2}$$

,

$$\begin{cases} A_i=\max(E) \\ B_i=0 \\ k=\dfrac{x_j-x_1}{x_2-x_1} \\ L(t)=A_i\cdot\sin(k\pi)\ \ (t=\pi) \end{cases} \tag{3}$$

,

$$\boldsymbol{P}=\boldsymbol{E}-\boldsymbol{L}(t) \tag{4}$$

,

where A_i and B_i are amplitudes of the harmonic function and n is the order of the polynomial. The first-order polynomial harmonic function $n=1$ is used to improve the computational efficiency and predict the nonlinear error. $\boldsymbol{E}$ is the nonlinear error value matrix, A_i is the maximum nonlinear error between two adjacent points, B_i is equal to zero, and k is the relative position of interpolation points on the whole path in Eq. (3). Meanwhile, $\boldsymbol{P}$ is the position point after compensation in Eq. (4).

Tool point data are applied to verify the Harmonic function algorithm as follows:

$\boldsymbol{p}_0$ =[-177.100 11.521 8.380]

$\boldsymbol{u}_0$ =[0.01205, -0.02112, 0.93240]

$\boldsymbol{p}_1$ =[-177.102, 13.735, 8.573]

$\boldsymbol{u}_1$ =[0.01225, -0.06738, 0.93552] .

Fig. 3 illustrates the nonlinear error prediction model. The similar prediction and actual error values verified the validity and accuracy of the error function expression.

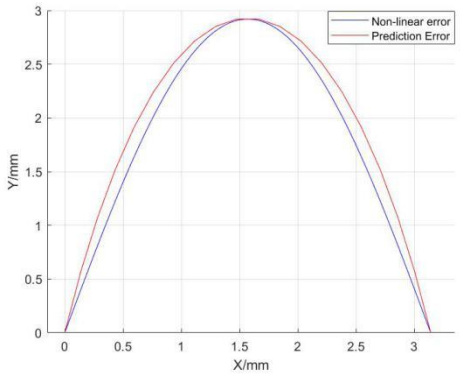

Fig. 3 Nonlinear error prediction model

The prediction error is used as the actual error compensation value, and the nonlinear error compensation mechanism is constructed to reduce the nonlinear error value. A section of the five-axis tool position file was used for the comparison of uncompensated and compensated tool trajectories. The comparison results are presented in Fig. 4a. The star-point curve represents the compensated tool trajectory, which approximates the ideal tool trajectory, while the curve with circles represents the uncompensated tool trajectory, which deviates significantly from the ideal trajectory. Fig. 4b shows the nonlinear error values of tool interpolation points without and with compensation. The results showed that nonlinear error values significantly reduce after compensation.

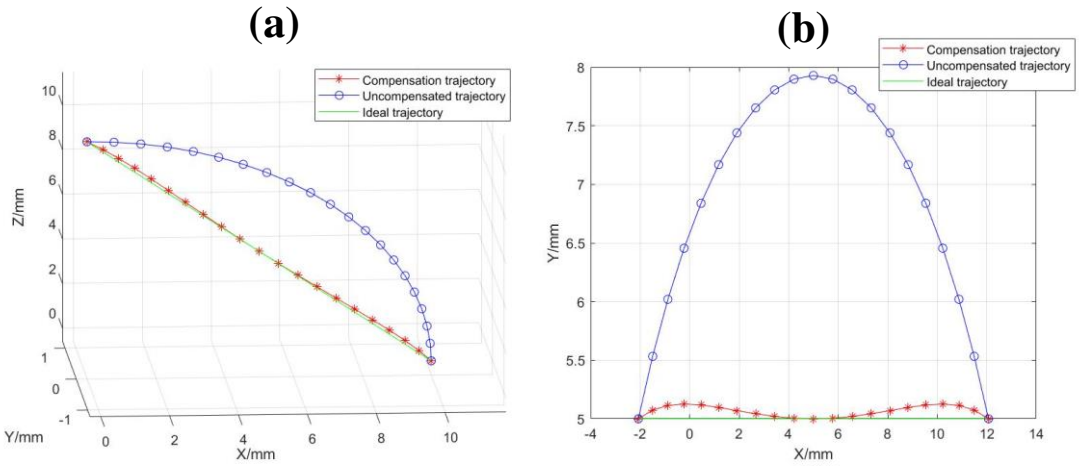

Fig. 4 Tool path and nonlinear error values. **a** Three-dimensional diagram. **b** Two-dimensional diagram

3.2 Local path tool profile optimization algorithm

Wang et al. [27] proposed a local path tool attitude optimization algorithm to address the phenomenon of overcutting caused by the sharp change of the cutter axis vector when the machining surface is located at the circular corner. The transformation matrix $O_wX_wY_wZ_w$ of the workpiece coordinate system shown in Fig. 5 is established. The specific steps are referred to in Reference [27].

$$\begin{cases} \boldsymbol{e}_x = \boldsymbol{V}_j \\ \boldsymbol{e}_y = (\boldsymbol{e}_y \times \boldsymbol{e}_z) \\ \boldsymbol{e}_z = (\boldsymbol{V}_j \times \boldsymbol{V}_{j+1}) \\ \boldsymbol{Lw} = \boldsymbol{E} \cdot \boldsymbol{Ln} \end{cases}, \tag{5}$$

where $\boldsymbol{V}_j$ and $\boldsymbol{V}_{j+1}$ are the starting and ending tool axis vectors, respectively; $\boldsymbol{Lw}$ is the original tool axis vector; $\boldsymbol{e}_x$, $\boldsymbol{e}_y$ and $\boldsymbol{e}_z$ are the X_0, Y_0 and Z_0 axes of the new coordinate system $O_wX_0Y_0Z_0$ respectively; $\boldsymbol{Ln}$ is the new tool axis vector; and $\boldsymbol{E}$ is the transformation matrix from the artifact coordinate system to the new coordinate system.

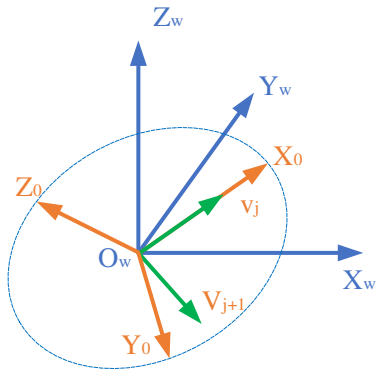

Fig. 5 Transformation diagram of cutter axis vector coordinates

Fig. 6 shows the diagram of the tool axis vector planning optimization algorithm, where $\boldsymbol{Q}(u)$ is the planning vector of adjacent points in the new coordinate system and $\phi_i(u)$ is the angle between the planning vector and the initial vector $\boldsymbol{V}_i$. The function expressions of vectors $\boldsymbol{Q}(u)$ and $\phi_j(u)$ given that the parameter u ranges from 0 to 1 are expressed as follows:

$$\boldsymbol{Q}(u) = \cos\phi_j(u) \cdot \boldsymbol{V}_j + \sin\phi_j(u) \cdot \boldsymbol{N}, \tag{6}$$

$$\phi_j(u) = \arccos(\boldsymbol{V}_j \cdot \boldsymbol{V}_{j+1}) \cdot u, \tag{7}$$

where $\boldsymbol{N}$ is the unit vector attached to axis Y_0 of the newly created transformation coordinate system and perpendicular to $\boldsymbol{V}_i$. $\boldsymbol{Q}(u)$ will reach the vector position $\boldsymbol{V}_{j+1}$ when u =1.

$$\boldsymbol{V}_{j+1} = \cos\phi_i(1) \cdot \boldsymbol{V}_i + \sin\phi_i(1) \cdot \boldsymbol{N} \tag{8}$$

Thus, $\boldsymbol{N}$ satisfies the following equation:

$$\boldsymbol{N}=\frac{\boldsymbol{V}_{j+1}-\cos\phi_j(1)\cdot\boldsymbol{V}_j}{\sin\phi_j(1)} \tag{9}$$

.

The following formula can be obtained when Eqs. (6) and (9) are combined:

$$\boldsymbol{Q}(u)=\left(\cos\phi_j(u)-\frac{\cos\phi_j(1)}{\sin\phi_j(1)}\sin\phi_j(u)\right)\cdot\boldsymbol{V}_j+\frac{\sin\phi_j(u)}{\sin\phi_j(1)}\cdot\boldsymbol{V}_{j+1} \tag{10}$$

.

According to Eq. (10), the tool axis vector planned in the new coordinate system is expressed as

$$\begin{cases}\boldsymbol{u}_j^{'}=\boldsymbol{Q}_1(u)\\ \boldsymbol{v}_j^{'}=\boldsymbol{Q}_2(u)\\ \boldsymbol{w}_j^{'}=\boldsymbol{0}\end{cases} \tag{11}$$

,

where the subscript number of $\boldsymbol{Q}(u)$ represents the column number of the vector. The optimized complement vector between adjacent tool axis vectors can be obtained by substituting Eq. (11) into Eq. (5).

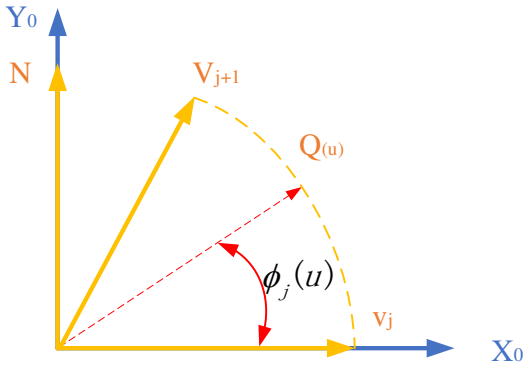

Fig. 6 Diagram of tool axis vector plane interpolation

The tool axis vector after linear interpolation deviates from the ideal position when an optimization measure is absent between two adjacent tool axis vectors. The tool axis vector is in an ideal state without any mutation phenomenon and generation of tool attitude error after applying the vector optimization algorithm. The results of comparative experiments are illustrated in Fig. 7. The experimental results showed that tool attitude optimization with local path can effectively compensate the abrupt change of tool axis vector direction or curvature radius.

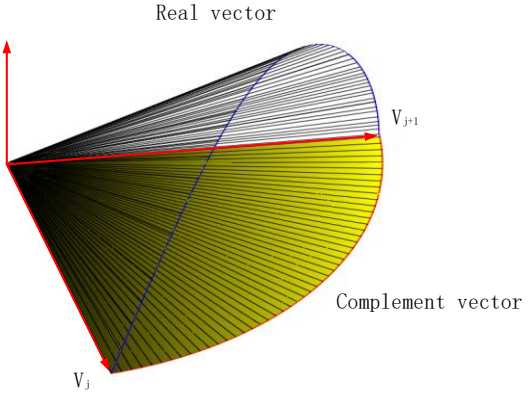

Fig. 7 Optimization comparison of the tool axis vector

4 Optimizing the compensation strategy

4.1 Influence of tool swing angle amplitude on nonlinear error

The division of surface processing area depends on properties of surface feature points and is mainly judged by the variation of the tool axis vector. According to Eq. (1), the change of the tool axis vector will lead to the change of rotation axis angle, that is, the amplitude of the tool swing angle. The amplitude of tool swing angle is regarded as the planning condition of surface feature points to simplify the calculation.

The relationship between the nonlinear error value and the angle of the rotating axis A and C are obtained according to the method used in Reference [22] to verify the correlation between the variation of the amplitude of the tool swing angle and the nonlinear error value as follows:

$$\varepsilon_j = \left| \frac{a-b-c}{d} \right|, \tag{12}$$

where

$$\begin{cases} a = \sin(A_j)\sin(A_{j+1})\cos((1-u)A_j + uA_{j+1})\sin(C_{j+1} - C_j) \\ b = \sin((1-u)A_j + uA_{j+1})\sin(A_{j+1})\cos(A_{j+1})\sin((1-u)(C_{j+1} - C_j)) \\ c = \sin((1-u)A_j + uA_{j+1})\cos(A_{j+1})\sin(A_{j+1})\sin(u(C_{j+1} - C_j)) \\ d = \sqrt{1-((\cos(A_j)\cos(A_j + \Delta A_j) + \sin(A_j)\sin(A_j + \Delta A_j)\cos(\Delta C_j))^2} \end{cases}, \tag{13}$$

$$\begin{cases} A_{j+1} = A_j + \Delta A_j \\ C_{j+1} = C_j + \Delta C_j \end{cases}, \tag{14}$$

where A_{j+1} and A_j are adjacent angles to the X-axis, C_{j+1} and C_j are adjacent angles to the Z-axis.

Eqs. (12) and (14) are simplified by setting $A_j = 0$ to obtain:

$$\varepsilon_j = \left|\sin(\Delta A_j / 2) \times \sin(\Delta C_j / 2)\right| \approx \left|\frac{1}{4}\Delta A_j \Delta C_j\right| . \tag{15}$$

Fig. 8 shows the relationship between nonlinear error values and the amplitude of the tool swing angle. The nonlinear error value is equal to zero and clearly belongs to triaxial machining when the amplitude of the tool swing angle is zero. A large amplitude of the tool swing angle corresponds to a large nonlinear error value when the swing angle of the two rotation axes changes from $-\pi / 2$ to $\pi / 2$. Therefore, avoiding excessive amplitudes of the adjacent tool swing angle is necessary to improve the machining quality.

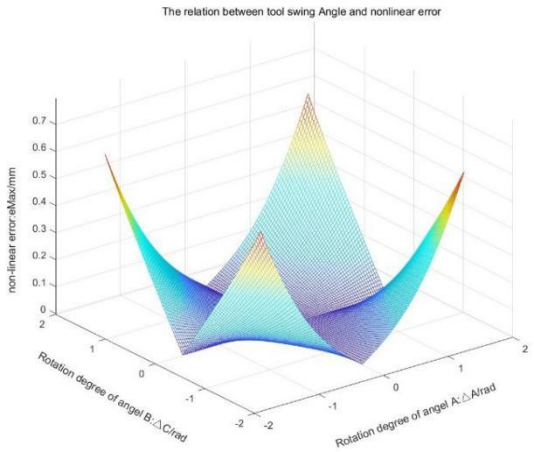

Fig. 8 Nonlinear error value and tool swing angle amplitude

4.2 Executing Strategy

As shown in Section 3.1, the change of tool axis vector can be judged according to the angle difference between adjacent rotation axes after transformation. The nonlinear error compensation and optimization measures for complex curved surfaces are shown in Fig. 9. The following boundary conditions of partition feature points are presented:

4.2.1 Rotation axis angle is equal

The interpolation mode between two points is a linear motion without nonlinear error when angles of adjacent rotation axes are equal. Hence, the compensation optimization algorithm is unnecessary. The following judgment formula is used to simplify the calculation:

$$\begin{cases} A_{n+1} - A_n = 0 \\ C_{n+1} - C_n = 0 \end{cases} \quad n = 1, 2, 3\mathrm{L}\ \ m-1 \tag{16}$$

.

4.2.2 Rotation axis angle is different

The boundary difference (set value is R) must be compared when the angle difference between adjacent rotation axes is set. If Eq. (17) is met, then the harmonic function method is adopted. If Eq. (18) is satisfied, then the local path tool pose optimization algorithm is adopted.

$$0<\left|A_{n+1}-A_n\right|\le R \text{ and } 0<\left|C_{n+1}-C_n\right|\le R \quad n=1,2,3\mathrm{L}\ \ m-1 \tag{17}$$

$$R<\left|A_{n+1}-A_n\right| \text{ or } R<\left|C_{n+1}-C_n\right| \quad n=1,2,3\mathrm{L}\ \ m-1 \tag{18}$$

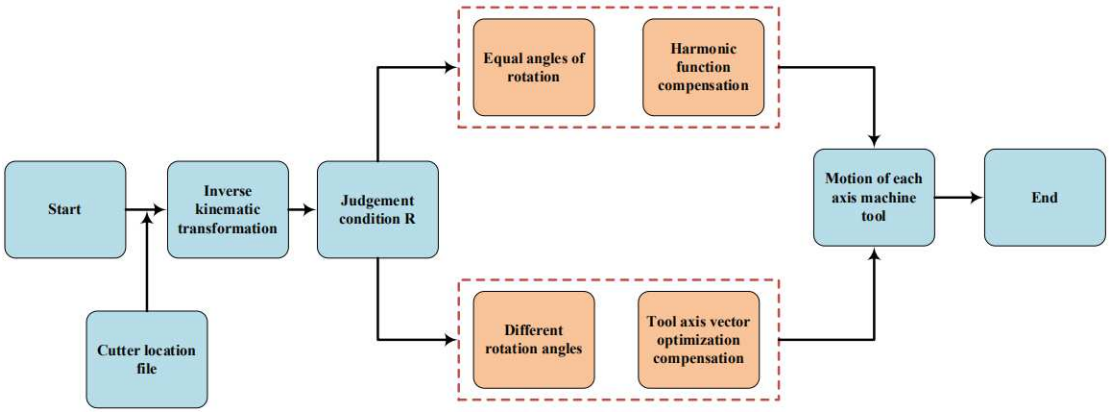

Fig. 9 Surface trajectory optimization process

4.3 Data simulation verification

The tool path of the blade cross section is examined to verify the effectiveness of the proposed method. Fig. 10 shows the diagram of the tool trajectory optimization plane for the blade part. The red curve is the original trajectory, and the dotted line is the compensation trajectory of the regional optimization algorithm. According to the execution strategy proposed in Section 3.2, the angle difference of the rotation axis of adjacent tool points on the blade trajectory was identified and assessed to obtain the four red-circle feature points in the figure. The blade trajectory was divided into four regions using feature points.

Areas A and B in Fig. 10 are used as an example. The angle difference between adjacent rotation axes at the corner of blade A satisfies Eq. (17). If the harmonic function algorithm is used to compensate, then the nonlinear error can be reduced to a certain extent. However, the overcutting problem may occur because whether or not the tool attitude is in a favorable cutting position is ignored. Therefore, the tool attitude optimization compensation algorithm is the ideal choice. Compensation diagram as shown in Fig. 11 for comparison of tool attitude optimization. The local amplification figure in Fig. 11a clearly showed that the blue cutter axis vector deviates from the ideal vector, and using local tool posture optimization algorithm the red cutter axis vector is in ideal plane, which can effectively correct the cutter axis vector processing mutation status, avoiding the phenomenon such as overcutting during the processing and Fig. 11b shows the compensation of the

nonlinear error values close to zero.

Fig. 10 shows that the angle interpolation of adjacent tool points on the back arc of blade B satisfies Eq. (16). If the tool attitude optimization algorithm is adopted, then the calculation amount of the program increases to a certain extent. Hence, the harmonic function compensation algorithm is adopted to achieve the optimal compensation effect. The compensation diagram is shown in Fig. 12 for tool trajectory comparison. Fig. 12a demonstrated that the compensation trajectory is close to the original trajectory when applying the harmonic function compensation mechanism and Fig. 12b shows the theoretical blue nonlinear error value after compensation is significantly less than 5×10^{-3} mm . Therefore, the nonlinear error regional compensation optimization algorithm can effectively identify feature points of the complex curved surface and the appropriate compensation algorithm is adopted to achieve a satisfactory compensation effect.

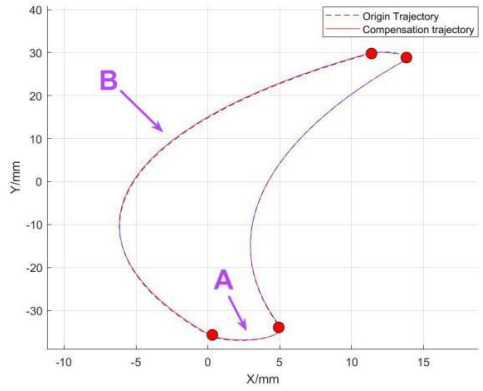

Fig. 10 Tool path of the blade part

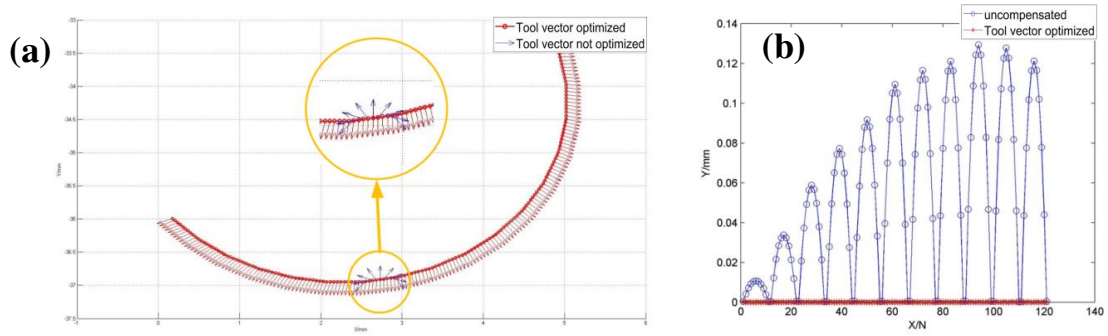

Fig. 11 Comparison of tool attitude optimization. **a**. Comparison of tool attitude. **b**. Comparison of nonlinear error values

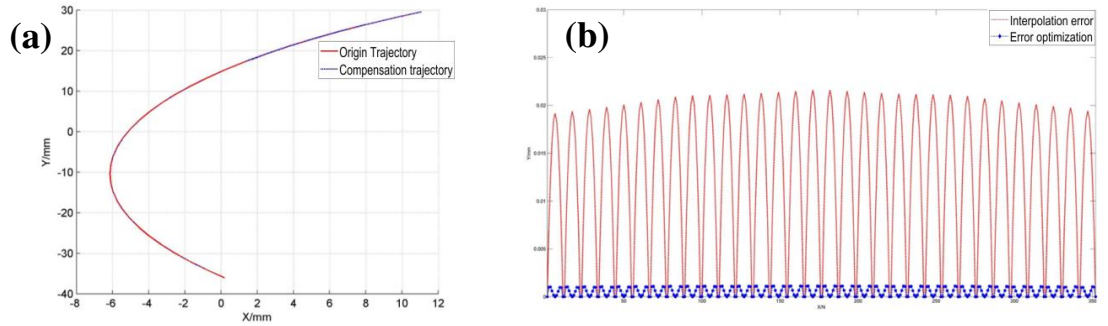

Fig. 12 Tool trajectory comparison. **a**. Comparison of trajectory. **b**. Comparison of nonlinear error values

5 Simulation and experiment

5.1 Experimental platform and specimen

The five-axis machine tool BV100 with double-swing table is used as the experimental platform in this study. According to the established kinematics model and the proposed nonlinear error regional compensation optimization algorithm, a special postprocessing software for BV100 five-axis machine tool is written in JAVA language. The software can directly transform the tool location source file into a part-processing program that can be recognized by the machine tool through postprocessing. The feature of the tool location can be judged in the postprocessing method, and the nonlinear error compensation can be automatically carried out according to the set decision boundary conditions. The operating interface of the postprocessing software is presented in Fig. 13.

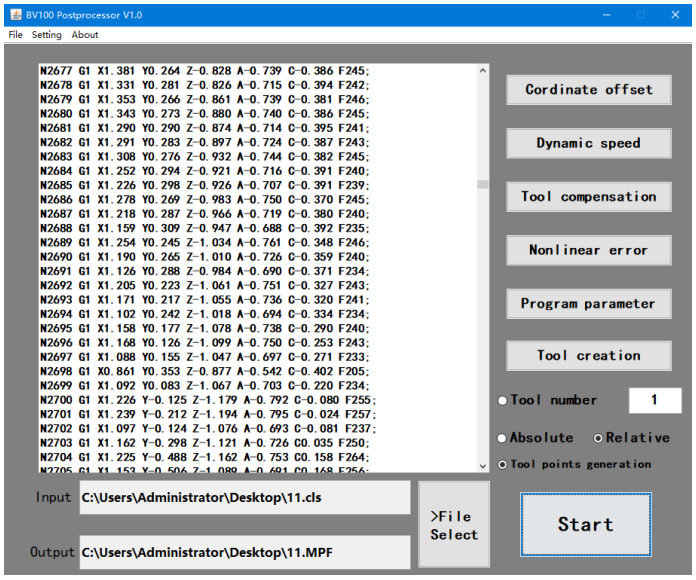

Fig. 13 BV100-dedicated postprocessing software

The turbine blade is used as a specimen in this study to demonstrate the nonlinear error compensation experiment given the typical complex curved surface of the turbine blade body. The selected blade profile is formed by fitting multiple sections, of which the theoretical size of section B is 0.65 mm for the inlet edge, 0.25 mm for the outlet edge, and 3.8 mm for the maximum thickness of the blade. The blade blank model adopts a cylindrical blank of $\phi 80 \times 220$ (actual cutting involves 600 series aluminum alloy 6061, with a composition of Mg1%, Si0.6%, Cu0.3%), and three kinds of cutting tools are used for processing. The following process route planning of the blade profile is established using the UG11.0 software platform:

(1) Step 1 (blade roughing). The rough shape of the model was milled with a three-axis linkage.

(2) Step 2 (semifinishing of blades). The blade profile is semifinished via five-axis radial spiral milling while leaving a finishing margin of 0.5 mm.

(3) Step 3 (blade finishing). The blades were finished using five-axis radial spiral milling and milling in place according to the theoretical size of the model.

5.2 Virtual Simulation

Cutting simulation can master the possible collision and interference phenomena in actual machining in advance. VERICUT simulation software developed by CGTech is used in this study for virtual machining. The VERICUT simulation software with functions of overcutting, interference inspection, program verification, and model measurement and analysis can accurately simulate the cutting of the tool and the movement of each axis of the machine tool in machining. The steps of simulation are as follows: First, establish of virtual machine. Machine model, control system, tool library, processing coordinate system, and other modules are set according to the characteristics of the BV100 machine tool. Second, processing preparation. A blank and NC program code are added and imported, respectively. Finally, start simulation process in the computer. The simulated cutting process is shown in Fig. 14. The absence of overcutting interference in the simulated cutting process indicated that the developed postprocessing software is effective and reliable.

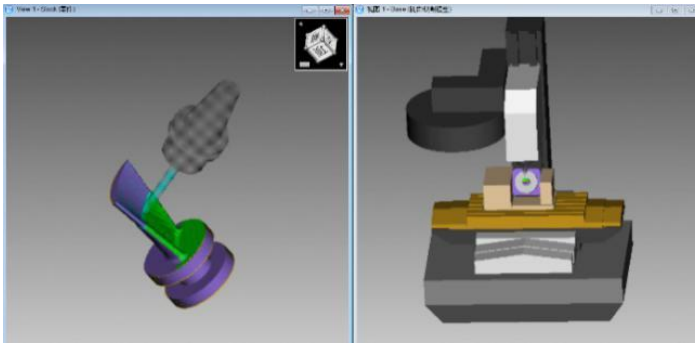

Fig. 14 BV100 simulation machining blade

Postprocessing of the program was carried out under the following conditions to verify the effectiveness of the proposed regional optimization strategy further during the blade finishing process in Section 4: (1) linear interpolation and (2) regional compensation optimization modes. The two NC codes after processing were simulated in VERICUT The results are illustrated in Fig. 15.

A public area with high identification of the blade, including the inner arc, back arc, and inlet and outlet steam edges of the blade, is selected in this study to compare the algorithms efficiently. The effects of the two processing methods were compared in terms of the number of point of out of tolerance (residual number), in which critical values of the residual height and overcutting were set to 0 mm. The distribution area of green residual and red overcut points on the virtual blade specimen picture evidently demonstrated that the optimization effect of regional compensation is better than that without compensation. The four evaluation criteria for the correlation of nonlinear errors after blade processing under different algorithms, namely, overcut number, maximum overcut value, residual number, and maximum residual value, are presented in Table 1. The four evaluation criteria reach the maximum value in the NC code without compensation. The overcutting phenomenon of inlet and outlet steam edges can be effectively eliminated when the regional optimization compensation algorithm is used. The simulation results proved the rationality and effectiveness of the proposed algorithm. Therefore, the developed BV100 special postprocessing software can be used in practical projects.

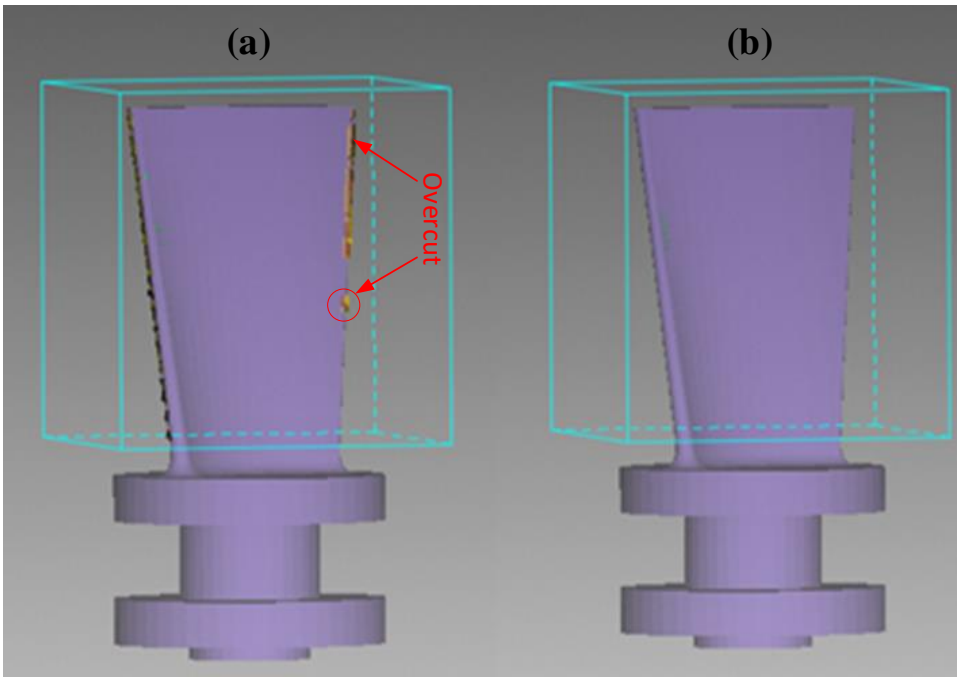

Fig. 15 Comparison of blade simulation processing. **a** Linear interpolation. **b** Regional compensation optimization

Table 1 Comparison of error data

Optimization algorithm	Linear interpolation	Regional compensation optimization
Number of overcutting (N)	228	0
Maximum overcut value (mm)	0.230206	0
Number of residual (N)	127	5
Maximum residual value (mm)	0.189351	0.125664

5.3 Cutting experiment

The processed NC code was verified using VERICUT simulation processing, and the correct NC code is imported into the BV100 five-axis CNC machine tool for experimental verification. The tool path is smooth without alarm, interference, or collision in the whole process of blade machining. However, machined parts must be measured to verify whether the process requirements are met. The process parameters are listed in Table 2, and the processing and results are illustrated in Fig. 16. The overall appearance of the blade contour before and after processing indicated a minimal difference. The local magnified contrast picture shown in Fig. 17 was obtained by magnifying and comparing the local position of the blade corner to analyze the difference in detail. The local comparison picture demonstrated that overcutting is present in the blade corner processed by the linear interpolation algorithm but absent in the blade processed via the regional optimization algorithm. Therefore, the blade profile processed with the compensation algorithm is clearly better than that without compensation.

Table 2 Process parameters

Process classification	Tool type	Tool diameter (mm)	Residual height (mm)	Allowance (mm)
Rough machining	End mill	30	0.2	1.5
Semifinishing	Ball-end	16	0.1	0.5
Finishing	Ball-end	10	0.1	0

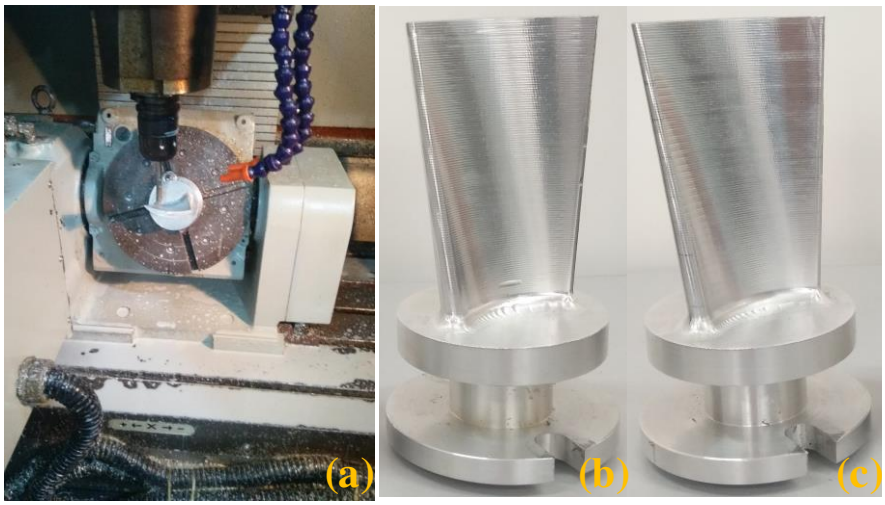

Fig. 16 Actual blade processing. **a** Machine process. **b** Linear interpolation. **c** Regional optimization.

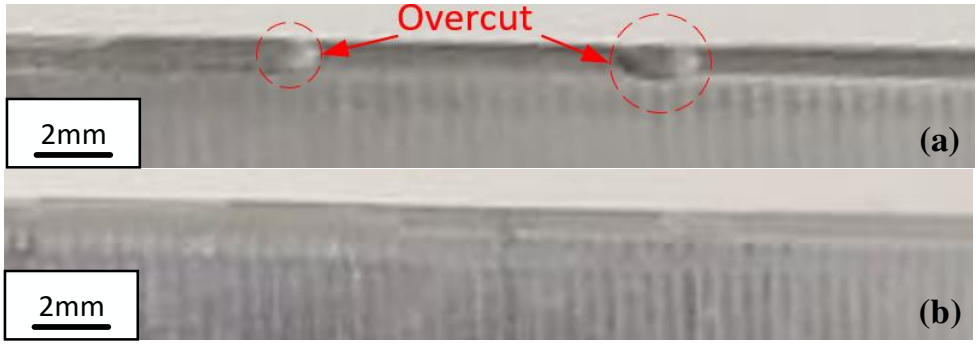

Fig. 17 Magnified comparison of blade corners. **a** Linear interpolation. **b** Regional optimization.

5.4 Measurement and analysis

Coordinate measuring machine(CMM) was used to measure the cross section of processed blades to verify the effectiveness of the nonlinear error regional compensation optimization algorithm. The results are shown in Fig. 18. The precision of several main features of the machined blade, such as maximum thickness, contour, inlet edge contour, and outlet edge contour, was measured.

The horizontal section A-A at the same place was measured using CMM to compare the processing results of linear interpolation and regional compensation optimization algorithm. The results are presented in Fig. 16. The profile of inlet and outlet edges of the blade without compensation machining is overcut. However, the regional compensation optimization algorithm

can effectively eliminate the overcutting problem of the inlet and outlet edge profile and meet the design requirements of the blade.

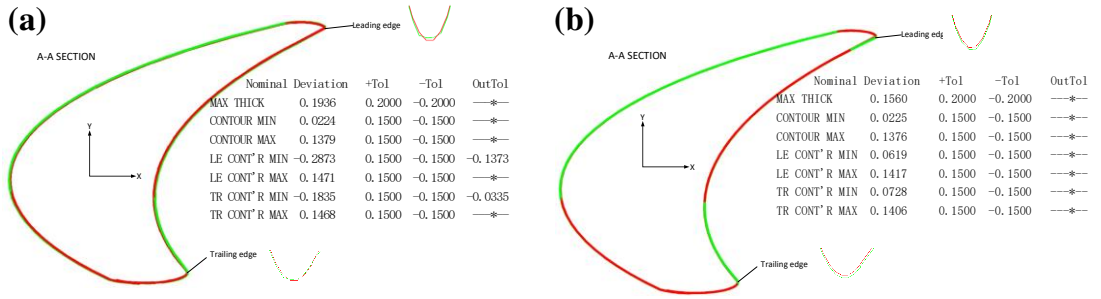

Fig.18 Measurement results of nonlinear error compensation. **a** Without compensation. **b** Regional compensation optimization.

Table 3 Nonlinear error values of different interpolation methods (mm)

NAME	MAX THICK	CONTOUR	LE CONT'R	TR CONT'R
Nominal Deviation	(-0.20–0.20)	(-0.15–0.15)	(-0.15–0.15)	(-0.15–0.15)
Without compensation	0.1936	(-0.0224–0.1379)	(-0.2873–0.1471)	(-0.1835–0.1468)
Compensation optimization	0.1560	(-0.0225–0.1376)	(-0.0619–0.1417)	(-0.0728–0.1406)

The analysis of data in Table 3 demonstrated that the maximum thickness, contour, and contour accuracy of inlet and outlet steam edges of the processed specimen significantly improved after the blade adopts the regional compensation optimization algorithm. The deviation in the maximum thickness accuracy reduces by 0.0376 mm relative to the linear interpolation method only when the contour accuracy deviation is similar. Compared with those of the linear interpolation method, the upper deviation value reduces by 0.0054 and 0.0062 mm and the lower deviation value reduces by 0.2254 and 0.1107 mm, respectively. The simulation and actual milling of the blades specimen verified that the regional compensation optimization algorithm is more effective than the linear interpolation method in solving the nonlinear error problem of complex curved surface parts.

6 Conclusion

A regional compensation optimization algorithm was proposed in this study to solve the nonlinear error problem in the machining of complex curved surface parts globally. The BV100 five-axis machine tool and turbine blade were used as the experimental platform and specimen, respectively, to verify the effectiveness of the algorithm. The following conclusions can be drawn from the experimental results:

1. The surface can be divided into different compensation methods according to characteristic discrimination conditions of the complex curved surface to compensate for nonlinear errors.

2. The curved surface can be divided into different feature areas and various compensation algorithms can be applied on the basis of the variation condition of the tool axis vector.

3. The nonlinear error of five-axis machining of the complex curved surface can be effectively solved globally using the regional compensation optimization algorithm while improving the machining quality on the basis of the postprocessing technology.

Funding This paper was supported by the National Natural Science Foundation of China (No. 52165054) and the Natural Science Foundation of Guangxi Province(No. 2020GXNSFAA159142, Grant No.2018GXNSFAA281273).

Authors' contributions Wei Wei: methodology, software development, verification of simulation, verification of experiment, detection analysis, writing—original draft, review and editing; Qingchun Tang: methodology, supervision, writing—review and editing; Yutao Wang: methodology, software development, verification of simulation, detection analysis; Taizi Wang Chenyang Zhang and YingGuang Pan: verification of experiment, detection analysis, writing—review and editing.

Code availability Not applicable.

Availability of data and materials Not applicable.

Declarations

Ethics approval The authors claim that the research in this paper is the authors' original work and has not been published nor has it been submitted simultaneously elsewhere.

Consent to participate Informed consent was obtained from all authors who participated in the study.

Consent for publication The authors have consented to publish the research article in the journal.

Conflict of interest The authors declare no competing interests.

References

1. Sun Y, Jia J, Xu J, Chen M, Niu J (2021) Path, feedrate and trajectory planning for free-from s urface machining: A state-of-the-art review. Chinese J Aeronaut 42(10):31-54. https://doi.org/1 0.1016/j.cja.2021.06.011
2. Tang QC, Yin SH, Chen FJ, Huang S, Luo H, Geng JX (2018) Development of a postprocessor for head tilting-head rotation type five-axis machine tool with double limit rotation axis. Int J Adv Manuf Tech 97(9-12):3523-3534. https://doi.org/10.1007/s00170-018-2195-3
3. Liu Y, Wan M, Xing W, Xiao Q, Zhang W (2018) Generalized actual inverse kinematic model for compensating geometric errors in five-axis machine tools. Int J Mech Sci 145:299-317. https://doi.org/10.1016/j.ijmecsci.2018.07.022
4. Li Z, Zhu L (2019) Compensation of deformation errors in five-axis flank milling of thin-wall ed parts via tool path optimization. Precision Engineering 55:77-87. https://doi.org/10.1016/j.p recisioneng.2018.08.010
5. Wang Z, Lin X, Shi Y (2020) Efficiently constructing collision-free regions of tool orientations

for holder in five-axis machining of blisk. Chinese J Aeronaut 33(10):2743-2756. https://doi.org/10.1016/j.cja.2020.05.032

6. Cripps RJ, Cross B, Hunt M, Mullineux G (2017) Singularities in five-axis machining: Cause, effect and avoidance. International Journal of Machine Tools and Manufacture 116:40-51. https://doi.org/10.1016/j.ijmachtools.2016.12.002
7. Tang Q C, Yin S H, Zhang G H and Luo H (2018) Post-processor development for a turning an d milling composite machine tool. Int J Adv Manuf Technol 95(1-4): 131-141. https://doi.org/1 0.1007/s00170-017-1139-7
8. Tajima S, Sencer B (2020) Real-time trajectory generation for 5-axis machine tools with singularity avoidance. CIRP Annals 69(1):349-352. https://doi.org/10.1016/j.cirp.2020.04.050
9. Ibaraki S, Yoshida I, Asano T (2019) A machining test to identify rotary axis geometric errors on a five-axis machine tool with a swiveling rotary table for turning operations. Precision Engineering 55:22-32. https://doi.org/10.1016/j.precisioneng.2018.08.003
10. He W, Lei M, Bin H (2009) Iso-parametric CNC tool path optimization based on adaptive grid generation. Int J Adv Manuf Tech 41(5-6):538-548. http://dx.doi.org/10.1007/s00170-008-1500-y
11. Ding S, Mannan M, Poo A, Yang D, Han Z (2003) The implementation of adaptive isoplanar tool path generation for the machining of free-form surfaces. Int J Adv Manuf Tech 26(7): 852-860. https://doi.org/10.1007/s00170-004-2058-y
12. Can A, Unuvar A (2010) A novel iso-scallop tool-path generation for efficient five-axis machin ing of free-form surfaces. Int J Adv Manuf Tech 51(9-12):1083-1098. http://dx.doi.org/10.100 7/s00170-010-2698-z
13. Lin Z, Fu J, Shen H, Gan W (2014) On the workpiece setup optimization for five-axis machini ng with RTCP function. Int J Adv Manuf Tech 74(1-4):187-197. http://dx.doi.org/10.1007/s00 170-014-5981-6
14. Zou X, Ding Y, Wang T, Sang Z, Xu H (2016) Research of RTCP function for five-axis machine tools based on low-cost embedded CNC system. Key Engineering Materials 693:1591-1597. http://dx.doi.org/10.4028/www.scientific.net/KEM.693.1591
15. Hongya F, Maoyue L, Yuan L and Zhijuan C (2011) Study on cross quadrant angle processing algorithm in five axis milling. Procedia Engineering 15: 861-865. https://doi.org/10.1016/j.pro eng.2011.08.159
16. Zhang H, Yang J, Jiang H, Yao X (2010) Real-time error compensation for the two turntable five-axis NC machine tools. Jixie Gongcheng Xuebao/Journal of Mechanical Engineering 46(21):143-148. http://dx.doi.org/10.3901/JME.2010.21.143
17. Shi Z, Ye W, Liang R (2017) Multi-axis synchronous interpolation feed rate adaptive planning with rotational tool center point function under comprehensive constraints. Adv Mech Eng 9(6): 1608-1612. http://dx.doi.org/10.1177/1687814017712415
18. Tutunea-Fatan O R, Bhuiya M S H (2011) Comparing the kinematic efficiency of five-axis machine tool configurations through nonlinearity errors. Computer-Aided Design 43(9): 1163-1172. https://doi.org/10.1016/j.cad.2011.05.003
19. Fu G, Fu J, Shen H, Yao X, Chen Z (2015) NC codes optimization for geometric error compensation of five-axis machine tools with one novel mathematical model. Int J Adv Manuf Tech 80(9-12):1879-1894. http://dx.doi.org/10.1007/s00170-015-7162-7
20. Wu D, Wang Y, Feng J, Yang J (2007) Analysis and control of the non-linear errors in five-axis

NC machining. Shanghai Jiaotong Daxue Xuebao/Journal of Shanghai Jiaotong University 41(10):1608-1612. https://doi.org/10.16183/j.cnki.jsjtu.2007.10.011

21. Yang X, Zhou Y, Chen Z, Wang F (2012) Analysis and control of tool path interpolation error in rotary axes motions of five-axis CNC milling. Jixie Gongcheng Xuebao/Journal of Mechanical Engineering 48(3):140-146. http://dx.doi.org/10.3901/JME.2012.03.140
22. Geng C, Wu Y, Qiu J (2018) Analysis of Nonlinear Error Caused by Motions of Rotation Axes for Five-Axis Machine Tools with Orthogonal Configuration. Mathematical Problems in Engineering 2018: ArticleID 6123596, 16 pages. http://dx.doi.org/10.1155/2018/6123596
23. Zhang K, Zhang L, Yan Y (2016) Single spherical angle linear interpolation for the control of non-linearity errors in five-axis flank milling. Int J Adv Manuf Tech 87(9-12):3289-3299. http://dx.doi.org/10.1007/s00170-016-8720-3
24. Li J, Zhouyang H, Lou Y (2013) Tool path optimization in postprocessor of five-axis machine tools. Int J Adv Manuf Tech 68(9-12):2683-2691. http://dx.doi.org/10.1007/s00170-013-4872-6
25. Wu J, Wang X, Zhou H, Fang H (2020) Nonlinear error compensation for five-axis machine tool with dual rotary table. Computer Integrated Manufacturing Systems, CIMS 26(5):1185-1190. http://dx.doi.org/10.13196/j.cims.2020.05.004
26. Li Y, Chen Y, Chen Q (2012) Research on nonlinear error analysis and overproof processing method in five-axis NC machining with dual turntable. Applied Mechanics and Materials (121-126):3662-3666. http://dx.doi.org/10.4028/www.scientific.net/AMM.121-126.3662
27. Wang Y, Tang Q, Zhou Z, Li G (2018) Optimization algorithm of tool axis vector interpolation in five-axis linkage. Surface Technology 47(7):90-95. http://dx.doi.org/10.16490/j.cnki.issn.1001-3660.2018.07.012
28. Xu R, Cheng X, Zheng G, Chen Z (2017) A tool orientation smoothing method based on machine rotary axes for five-axis machining with ball end cutters. Int J Adv Manuf Tech 92(9-12):3615-3625. http://dx.doi.org/10.1007/s00170-017-0403-1
29. Lee Y (1997) Admissible tool orientation control of gouging avoidance for 5-axis complex sur face machining. CAD Computer Aided Design 29(7):507-521. http://dx.doi.org/10.1016/S0010-4485(97)00002-X
30. Tang Q, Yin S, Zhang Y, Wu J (2018) A tool vector control for laser additive manufacturing in five-axis configuration. Int J Adv Manuf Technol 98(5-8): 1671-1684. http://dx.doi.org/10.1007/s00170-018-2177-5
31. Ma J-w, Hu G-q, Qin F-z, Su W-w, Jia Z-y (2018) Optimization method of tool axis vector based on kinematical characteristics of rotary feed axis for curved surface machining. Int J Adv Manuf Technol 100(5-8): 2007-2020. http://dx.doi.org/10.1007/s00170-018-2738-7
32. Mi Z, Yuan C-M, Ma X, Shen L-Y (2017) Tool orientation optimization for 5-axis machining with C-space method. Int J Adv Manuf Technol 88(5): 1243-1255. https://doi.org/10.1007/s00170-016-8849-0
33. Fan L, Qi D, Shen B, Zhu Z (2011) Plane interpolation of tool orientation algorithm for 5-axis circumference milling. Jixie Gongcheng Xuebao/Journal of Mechanical Engineering 47(19):158-162. http://dx.doi.org/10.3901/JME.2011.19.158
34. Geng C, Yu D, Zhang H (2013) Tool orientation smooth interpolation algorithm for five-axis CNC machining. Jixie Gongcheng Xuebao/Journal of Mechanical Engineering 49(3):180-185. http://dx.doi.org/10.3901/JME.2013.03.180

35. Hong X, Hong R, Lin X (2019) Tool orientations generation and nonlinear error control based on complex surface meshing. Int J Adv Manuf Tech 105(10):4279-4288. http://dx.doi.org/10.1007/s00170-019-04480-w

Supplementary Files

This is a list of supplementary files associated with this preprint. Click to download.

- JAVAPostProcessorCode.docx